

## Modulation of Microenvironment Acidity Reverses Anergy in Human and Murine Tumor-Infiltrating T Lymphocytes

Arianna Calcinotto<sup>1,5</sup>, Paola Filipazzi<sup>3</sup>, Matteo Grioni<sup>1</sup>, Manuela Iero<sup>3</sup>, Angelo De Milito<sup>6,7</sup>, Alessia Ricupito<sup>1</sup>, Agata Cova<sup>3</sup>, Rossella Canese<sup>6</sup>, Elena Jachetti<sup>1</sup>, Monica Rossetti<sup>3</sup>, Veronica Huber<sup>3</sup>, Giorgio Parmiani<sup>2</sup>, Luca Generoso<sup>1</sup>, Mario Santinami<sup>4</sup>, Martina Borghi<sup>6</sup>, Stefano Fais<sup>6</sup>, Matteo Bellone<sup>1</sup>, and Licia Rivoltini<sup>3</sup>

### Abstract

Stimulating the effector functions of tumor-infiltrating T lymphocytes (TIL) in primary and metastatic tumors could improve active and adoptive T-cell therapies for cancer. Abnormal glycolysis, high lactic acid production, proton accumulation, and a reversed intra-extracellular pH gradient are thought to help render tumor microenvironments hostile to roving immune cells. However, there is little knowledge about how acidic microenvironments affect T-cell immunity. Here, we report that lowering the environmental pH to values that characterize tumor masses (pH 6–6.5) was sufficient to establish an anergic state in human and mouse tumor-specific CD8<sup>+</sup> T lymphocytes. This state was characterized by impairment of cytolytic activity and cytokine secretion, reduced expression of IL-2R $\alpha$  (CD25) and T-cell receptors (TCR), and diminished activation of STAT5 and extracellular signal-regulated kinase (ERK) after TCR activation. In contrast, buffering pH at physiologic values completely restored all these metrics of T-cell function. Systemic treatment of B16-OVA-bearing mice with proton pump inhibitors (PPI) significantly increased the therapeutic efficacy of both active and adoptive immunotherapy. Our findings show that acidification of the tumor microenvironment acts as mechanism of immune escape. Furthermore, they illustrate the potential of PPIs to safely correct T-cell dysfunction and improve the efficacy of T-cell-based cancer treatments. *Cancer Res*; 72(11); 2746–56. ©2012 AACR.

### Introduction

Several lines of evidence suggest that T-cell immunity may play a role in controlling tumor development. Tumor-infiltrating T lymphocytes (TIL) with an effector/memory phenotype are associated with a more favorable prognosis in patients with cancer (1) and mediate tumor regression when adoptively transferred after *ex vivo* activation (2). However, TILs are reported to acquire functional defects at the tumor site and enter a state of reversible anergy, mostly attributed to subop-

timal T-cell receptor (TCR) ligation, a lack of TCR and CD8 colocalization, or inhibitory signaling through CTLA4 (3–5). This may, at least in part, explain the clinical observation that TILs can be abundantly detected in progressing cancer lesions (6).

An issue frequently neglected relates to the metabolic features of the tumor microenvironment, which represents a potentially hostile milieu due to the hypoxic and acidic conditions that occur as a consequence of inadequate blood flow, inflammation, enhanced glycolysis (the so-called Warburg effect), and the production of acidic metabolites (7). In addition, excessive CO<sub>2</sub> release caused by altered glycolysis leads to increased tumor expression of carbonic anhydrase IX (CA-IX), thus contributing to further acidification of the extracellular tumor environment (8, 9). Hypoxia also activates the hypoxia-inducible factor (HIF) pathway, which in turn upregulates glucose transporters and CA-IX and leads to additional exacerbation of tumor acidosis (8). As a result, the extracellular pH can drop to values of 6.0 or less and is on average 0.2 to 1.0 units lower than that of normal tissues (10, 11). This biochemical shift has been shown to provide a selective growth advantage to tumor cells (7) at the expense of infiltrating host cells, including immune cells. While the impact of these metabolic alterations on TILs is presently unknown, the clinical evidence that metabolic acidosis is often associated with immunodeficiency (12), and that both leukocyte activation and the bactericidal capacity of leukocytes are generally impaired at reduced pH (13), suggests that T cells could be extremely sensitive to pH variations.

**Authors' Affiliations:** <sup>1</sup>Cellular Immunology Unit, <sup>2</sup>Immuno-biotherapy of Melanoma and Solid Tumors, San Raffaele Scientific Institute; <sup>3</sup>Unit of Immunotherapy of Human Tumors, <sup>4</sup>Melanoma and Sarcoma Unit, Fondazione IRCCS Istituto Nazionale dei Tumori; <sup>5</sup>Università Vita-Salute San Raffaele, Milan; <sup>6</sup>Department of Therapeutic Research and Medicines Evaluation, Unit of Antitumor Drugs, Istituto Superiore di Sanità, Rome, Italy; and <sup>7</sup>Department of Oncology-Pathology, Cancer Center Karolinska, Karolinska Institute, Stockholm, Sweden

**Note:** Supplementary data for this article are available at Cancer Research Online (<http://cancerres.aacrjournals.org/>).

A. Calcinotto, P. Filipazzi, M. Bellone, and L. Rivoltini contributed equally to this work.

**Corresponding Authors:** Licia Rivoltini, Unit of Immunotherapy of Human Tumors, Fondazione IRCCS Istituto Nazionale dei Tumori, via G. Venezian 1, Milan 20133, Italy. Phone: 39-02-2390-3245; Fax: 39-02-2390-2154; E-mail: [licia.rivoltini@istitutotumori.mi.it](mailto:licia.rivoltini@istitutotumori.mi.it); and Matteo Bellone, Cellular Immunology Unit, San Raffaele Scientific Institute, via Olgettina 58, Milan 20132, Italy. Phone: 39-02-2643-4789; Fax: 39-02-2643-4786; E-mail: [bellone.matteo@hsr.it](mailto:bellone.matteo@hsr.it)

doi: 10.1158/0008-5472.CAN-11-1272

©2012 American Association for Cancer Research.

Here, we report that relatively minor changes in the extracellular pH promote reversible anergy associated with impaired effector functions in both human and mouse tumor-specific CD8<sup>+</sup> T lymphocytes. Buffering low pH at the tumor site by *in vivo* administration of the proton pump inhibitor (PPI) esomeprazole improved TIL efficacy and delayed cancer progression in tumor-bearing mice. These data highlight tumor acidity as a novel mechanism of immune escape that could be targeted for rescuing effective tumor immunity and achieving disease control in patients with cancer.

## Materials and Methods

### Phenotypic and functional studies of human TILs

TILs were isolated and cultured as previously described (14), stained with the indicated monoclonal antibodies (mAb; BD Biosciences) and analyzed with a FACSCalibur (BD Biosciences) and FlowJo Software (Tree Star Inc.). TILs were assessed for tumor recognition by IFN $\gamma$  ELISpot assays (15). TIL were stimulated with Dynabeads CD3/CD28 T Cell Expander (1:20 ratio; Invitrogen Dynal AS) for 72 hours at the indicated pH and then assessed for proliferation by carboxy-fluorescein succinimidyl ester (CFSE; CellTrace CFSE Cell Proliferation Kit; Molecular Probes). For cytokine secretion analysis, TILs were cultured at the indicated pH for 3 days and then stimulated with CD3/CD28 T Cell Expander beads (1:20 ratio) or with autologous tumor cells (8:1 ratio). Twenty-four-hour supernatants were tested using FlowCytomix Human Th1/Th2 multiplex kit (Bender MedSystems). Data were analyzed by FlowCytomix Pro 2.2 software (Bender MedSystems). The IL-2R  $\alpha$ -chain was analyzed using an anti-CD25 mAb (BD Biosciences) on TILs stimulated for 24 hours with Dynabeads CD3/CD28 beads (1:20 ratio). CD3- $\zeta$ chain and perforin levels (detected after 6 hours of incubation with autologous tumor cells, 8:1 ratio) were evaluated by flow cytometry. For Annexin-V/propidium iodide (PI) studies, TILs were cultured for 3 days at the indicated pH and then stained with the rhAnnexin V-FITC Kit (Bender MedSystems). For intracellular phospho-protein analysis, TILs were stimulated with an anti-CD3 mAb (2  $\mu$ g/mL, 5 minutes; OKT3, Orthoclone; Janssen-Cilag) or IL-2 (150 ng/mL, 30 minutes; Proleukin, Chiron Corp.). Cells were then fixed, permeabilized, and stained by anti-ERK (pT202/pY204) or anti-STAT5 (pY694) mAbs (BD Biosciences).

No detrimental effect of low pH on either mAb binding activity or cytokine detection was observed. Melanoma cell lines, authenticated and characterized according to UKCCR guidelines (16), were obtained from patients after informed consent and ethical committee approval.

### Animals and tumor cell lines

C57BL/6J (Charles River) and C57BL/6-Tg(Tcr $\alpha$ Tcr $\beta$ ) 425Cbn/J (OTI) female mice (17) were treated in accordance with the European Community guidelines. B16F1 melanoma (American Type Culture Collection; ATCC) and RMA thymoma cells (18) were maintained in RPMI-1640 plus 10% heat-inactivated fetal calf serum (FCS). For B16-OVA cells (19), the medium was supplemented with hygromycin (100  $\mu$ g/mL).

### Immunization procedures

Dendritic cells (DC; ref. 20) were incubated for 60 minutes at 37°C with 2  $\mu$ g/mL of OVA<sub>257–264</sub> (21), TRP-2<sub>180–188</sub> (ref. 22; Proimmune), or STEAP<sub>186–193</sub> (23), and injected intradermally ( $5 \times 10^5$ /mouse). Esomeprazole was administered intraperitoneally (i.p.; 12.5 mg/kg; AstraZeneca).

### OTI cells

Day 5 RAG<sup>−/−</sup> OTI CD8<sup>+</sup> T blasts (20), which were cultured for the previous 24 hours at pH 5.5 to 7.4, were stimulated with phorbol myristate acetate (PMA; 60 ng/mL) and ionomycin (1  $\mu$ g/mL) and assessed for intracellular cytokine production (20) or for cytolytic activity by <sup>51</sup>Cr release assay (19). Lytic units (LU) were determined as the number of effector cells capable of killing 50% (LU<sub>50</sub>) of the target cells. Cells cultured at pH 7.4 were also CFSE-labeled (20) and injected i.v.

### STEAP-specific T cells

Splenocytes from C57BL/6 mice vaccinated with STEAP<sub>186–193</sub>-pulsed DCs were specifically restimulated *in vitro* and, after an additional day of culture at pH 6.5 or 7.4 (day 5), were either counted by trypan blue exclusion or assessed for intracellular cytokine production (20).

### Tumor implantation, processing, and flow cytometric analyses

Mice were challenged s.c. with  $2 \times 10^5$  B16-OVA or  $5 \times 10^4$  B16F1 cells. When needed, B16 melanoma-bearing mice were sublethally irradiated (600 rad) and, the day after, were infused (i.v.) with  $60 \times 10^6$  splenocytes derived from female donors presensitized 1 week before against tyrosinase-related protein 2 (TRP-2) antigen (21). In survival experiments, tumor size was evaluated *in vivo* by measuring 2 perpendicular diameters by a caliper; animals were sacrificed when lesions reached  $\geq 10$  mm diameter. To analyze immune cell infiltrate, animals were killed and tumors were excised, skinned and wet weighed (g) before processing. They were disaggregated and digested in collagenase D for 1 hour at 37°C to obtain single-cell suspension. Live cells were counted by trypan blue exclusion and stained for flow cytometric analysis. Data concerning the frequency and absolute numbers of different cell subsets analyzed were reported as referred to grams of tumor wet weight. Single-cell suspensions were assessed for phenotype, whereas intracellular cytokine production was evaluated after stimulation with PMA/ionomycin. For phospho-protein cytofluorimetric analysis, TILs were stimulated 20 minutes with PMA (200 ng/mL), fixed, permeabilized, and stained with anti-ERK (pT202/pY204) mAb. Data were analyzed by FlowJo software (Tree Star Inc.), gating on low physical parameters that select for lymphocytes. An additional gate was generated within the CD8<sup>+</sup>CD44<sup>+</sup> T cells, and cells were next analyzed for the expression of CFSE and/or IFN $\gamma$ . The absolute cell number of each subset in the serial gates was calculated by multiplying the number of gated cells by their percentage in the total cell population. In some experiments, CD8<sup>+</sup> cells were purified with anti-mouse CD8 MicroBeads (Miltenyi Biotec) and intracellular IFN $\gamma$  production was assessed in the presence of target

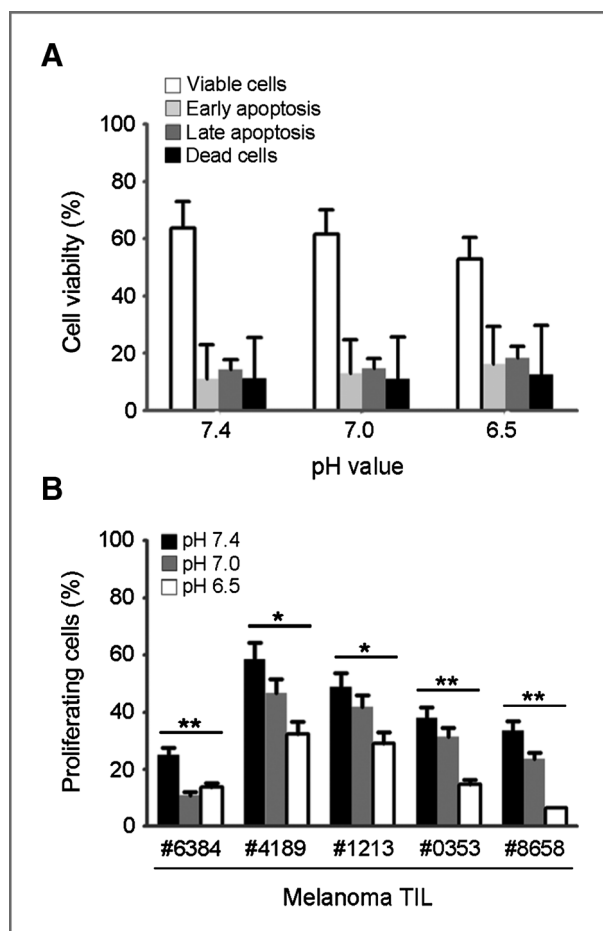


**Figure 1.** Low pH induces a defect in TIL proliferation without affecting cell viability. **A**, melanoma TILs ( $n = 5$ ) were cultured for 3 days at the indicated pH values and then evaluated for viability by Annexin-V/PI staining. Data represent the mean  $\pm$  SD. **B**, the same TILs were also tested for their proliferative activity in the presence of CD3/CD28 beads (TIL:beads = 20:1) by CFSE. Data represent mean  $\pm$  SD of triplicate determinations. \*,  $P < 0.05$ ; \*\*,  $0.01 < P < 0.001$  (the Student  $t$  test).

cells unpulsed or pulsed with increasing concentrations of OVA<sub>257–264</sub> peptide.

### **In vivo magnetic resonance spectroscopy**

*In vivo* measurements of tumor pH were conducted by  $^{31}\text{P}$  magnetic resonance spectroscopy (MRS) using the exogenous cell-impermeable pH reporter 3-aminopropyl phosphonate (3-APP). The extracellular pH (pHe) value was measured from the chemical shift difference between the 3-APP resonance and that of  $\alpha$ -ATP at  $-7.57$  ppm. B16-OVA-bearing mice underwent MRI/MRS examination once the tumor reached a volume of 300  $\mu\text{L}$ . The 3-APP probe was administered i.p. (128 mg/kg) immediately before MRI/MRS analysis. Esomeprazole was administered i.p. (12.5 mg/kg), and examinations occurred at times ranging from 20 minutes to 6 hours. Data analysis and technical procedures have been previously described in detail (10).

### **Statistics**

Statistical analyses were conducted using the unpaired Student  $t$  test or the log-rank test (survival curves) with Prism 5 software (GraphPad Software).  $P$  values less than 0.05 were considered statistically significant.

### **Results**

#### **Acidic pH induces reversible anergy in TILs**

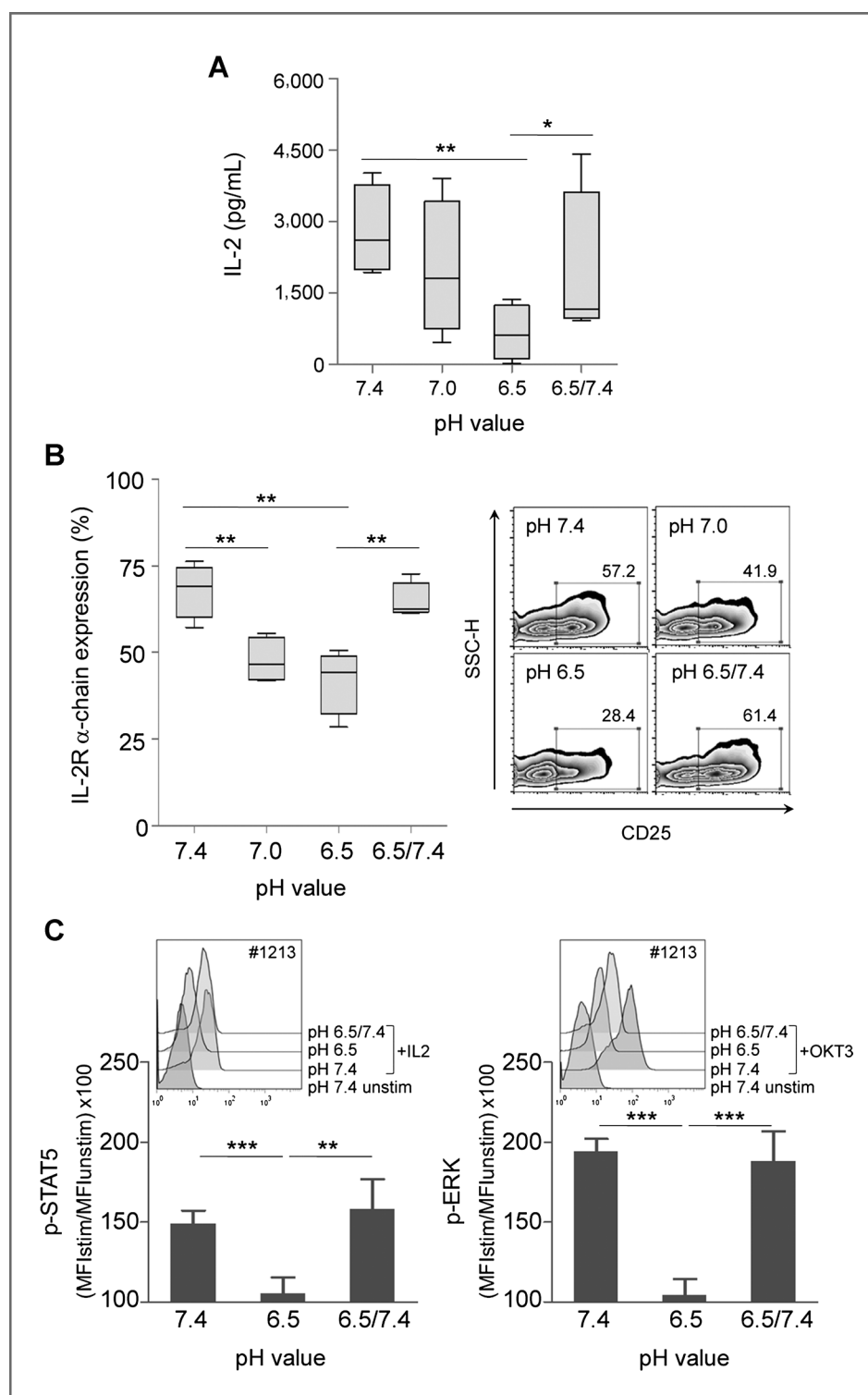
To test the effects of pH alterations on the proliferative and functional properties of tumor-specific T cells, we selected TILs (ref. 14; Supplementary Table S1) able to specifically recognize autologous melanoma cells (Supplementary Fig. S1). To mimic pH conditions at the tumor site, TILs were cultured at pH ranging from 7.4 to 6.5 for 3 days, as previous experiments showed that longer exposure was associated with significant apoptosis. After 3 days of culture, Annexin-V/PI staining showed no major change in the percentage of early or late apoptotic cells at pH 7.0 or 6.5 relative to pH 7.4 (Fig. 1A). TILs proliferative activity, evaluated by CFSE dye dilution following CD3/CD28 stimulation, was significantly decreased at pHs lower than physiologic levels in all cases, with a mean inhibition of 30% (with a range of 14%–54%) and 56% (with a range of 40%–90%) at pH 7.0 and 6.5, respectively (Fig. 1B). Similar data were obtained using CD3<sup>+</sup> T cells from healthy donors or Ag-specific CD8<sup>+</sup> T lymphocytes from patients with melanoma, suggesting this is a more general response of T cells to unfavorable pH conditions rather than a specific TIL feature (Supplementary Fig. S2).

Impaired proliferation in the absence of apoptosis at acidic pH levels suggested the onset of anergy. Indeed, IL-2 secretion in response to mitogenic stimuli, a feature typically tested for assessing T-cell anergy (24), was strongly affected in TILs maintained for 3 days at an acidic pH (Fig. 2A). Interestingly, IL-2 production (Fig. 2A), as well as proliferative activity (data not shown), were restored when TILs first cultured in pre-conditioned medium (pH 6.5), were then returned to physiologic pH (7.4) for 24 hours before the assay, suggesting that the phenomenon is reversible at least under these experimental conditions. CD25 expression, upon CD3/CD28 stimulation, was also progressively affected by culturing TILs at decreasing pH levels, and expression was similarly reversed by physiologic pH buffering for 24 hours (Fig. 2B).

Anergic T cells may have compromised JAK3/STAT5 pathway signaling (25) and reduced activation of extracellular signal-regulated kinase (ERK; ref. 26). Correspondingly, STAT5 and ERK phosphorylation in response to IL-2 or OKT3 activation, respectively, was completely abrogated in TILs following 3 days of culture at pH 6.5, whereas a full recovery was obtained by pH buffering for an additional 24 hours (Fig. 2C). A tendency to decrease CD3 and  $\zeta$ -chain expression, another feature of T cells in patients with cancer (27), was in addition observed upon TIL culturing at a low pH (Supplementary Fig. S3).

Perforin degranulation and IFN $\gamma$ , TNF- $\alpha$ , and IL-2 release in response to autologous tumor cells were significantly impaired at pH 6.5, although these functions were restored with additional 24-hour incubation at physiologic pH (Fig. 3).

**Figure 2.** Low pH induces a deficit in IL-2 secretion and IL-2R  $\alpha$ -chain (CD25) expression and impairs STAT5 and ERK activation in melanoma TILs. Melanoma TILs were cultured at the indicated pH values. A and B, at day 3, lymphocytes were stimulated with CD3/CD28 beads (TIL:beads = 20:1) to assess IL-2 production (A) and CD25 expression (B). Bars, box-and-whisker diagrams ( $n = 5$ ). Horizontal line, median. As a representative example, TIL dot plots (#0353) are shown with numbers indicating the percentage of cells expressing CD25 (B, right). C, the same TILs were evaluated by flow cytometry for STAT5 and ERK activation upon IL-2 (150 ng/mL, left) or OKT3 (2  $\mu$ g/mL, right) stimulation. As representative example, TIL histogram plots (#1213) are shown. Data represent mean  $\pm$  SD. In all experiments, TILs restored to pH 7.4 for 24 hours before the assay (6.5/7.4 in A–C) were also included in the analysis. \*,  $0.05 < P < 0.01$ ; \*\*,  $0.01 < P < 0.001$ ; \*\*\*,  $P < 0.001$  (the Student  $t$  test).



The detrimental impact of low pH on T-cell activity was not due to the effects of pH on the tumor target cells, as these cells did not change their surface expression of human leukocyte antigen (HLA) class I, tumor antigens (Supplementary Fig. S4A), or the HLA/peptide complexes recog-

nized by the Ag-specific T cells under low pH conditions (Supplementary Fig. S4B). Taken together, these data show that acidic pH conditions resembling those observed in tumor lesions promote a reversible anergic state in human TILs, probably due to downregulation of the high affinity

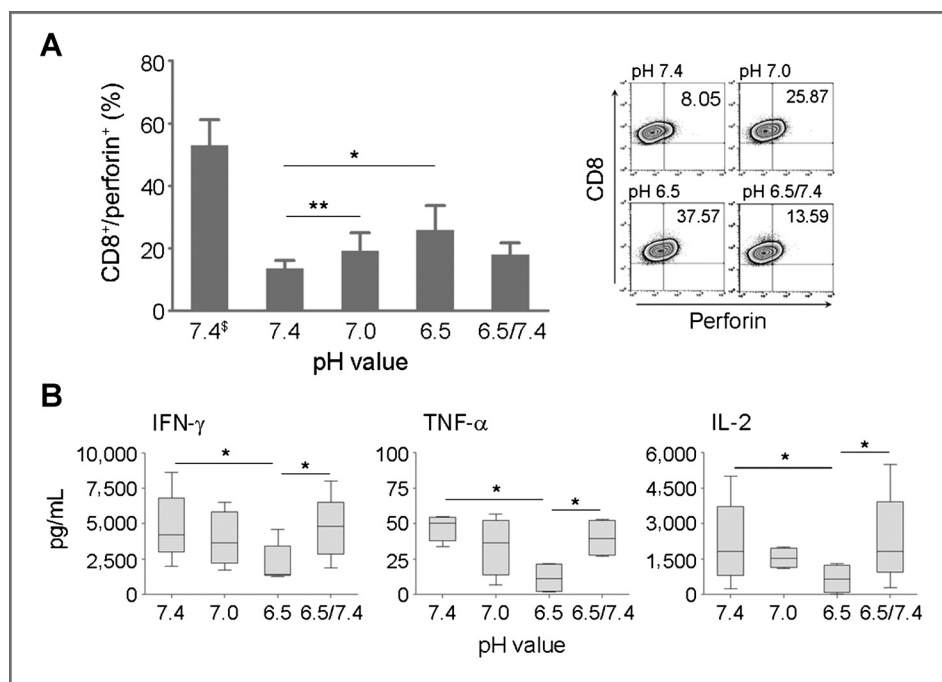


**Figure 3.** Low pH compromises the effector function of melanoma TILs. **A**, melanoma TILs ( $n = 5$ ) were cultured at the indicated pH values. At day 3, lymphocytes stimulated with autologous tumor cells (TIL:tumor = 8:1) were tested for perforin release by intracellular staining. Data represent mean  $\pm$  SD.  $\S$ , TILs cultured with medium alone. As representative example, TIL dot plots (#8658) are shown with numbers indicating the percentage of CD8<sup>+</sup>/perforin<sup>+</sup> T cells (right). **B**, IFN $\gamma$ , TNF- $\alpha$ , and IL-2 release by TILs after a 24-hour incubation with autologous tumor cells (TIL:tumor = 8:1). Bars, box-and-whisker diagrams ( $n = 5$ ). Horizontal line, median. In all experiments, T cells exposed to pH 7.4 for 24 hours before the assay were also included in the analysis (6.5/7.4 in **A** and **B**). \*,  $P < 0.05$ ; \*\*,  $0.01 < P < 0.001$  (the Student  $t$  test).

IL-2 receptor (CD25) and perturbation of the STAT5 and ERK pathways.

#### Effector functions of murine T lymphocytes are also affected by low pH

To investigate the sensitivity of murine T lymphocytes to acidic pH, *in vitro* primed OTI cells (20) were cultured for 24 hours at pH ranging from 5.5 to 7.4 and assessed for their viability. At pH less than 6.5 most of the cells died, whereas more than 80% survival was observed at pH 6.5 (Fig. 4A). Upon antigen stimulation, cytolytic activity, as well as IFN $\gamma$  and IL-2 release (Fig. 4B and C), were substantially reduced. As for human TILs (Figs. 2 and 3), the low pH-associated reduction in cytokine secretion by OTI cells was reversed by pH buffering (Fig. 4C). CD3 and TCR expression were also significantly downregulated in OTI cells exposed to pH 6.5 (Fig. 4D) and again fully recovered upon pH adjustment, corresponding with the trend observed in human TILs (Supplementary Fig. S3). Also in line with the human data, acidity-mediated functional impairment could be reproduced as well in spleen T cells from mice sensitized against the natural tumor antigen STEAP (Supplementary Fig. S5).

#### High-dose esomeprazole mediates buffering of tumor pH, improving TIL effector functions

To investigate whether tumor pH buffering could result in improved T-cell function *in vivo*, we first evaluated the pH value of tumor masses by MRS in mice challenged s.c. with B16-OVA melanoma cells. Mice were then treated with a high dose of esomeprazole (12.5 mg/kg), a PPI used as a standard therapy for neutralization of gastric acid that has been shown to increase tumor pH in human melanoma xenografts (10). The impact of PPI treatment on tumor pH was then evaluated.

MRI T2-weighted images of a B16-OVA s.c. xenograft show homogeneity in the vast majority of the tumor mass and in all sections examined, with absence of hyperintense areas or hypointense areas (Fig. 5A). Under these conditions it is reasonable to assume that pH is also homogeneous. At baseline, the tumor pH value was approximately 6.5, whereas PPI therapy caused a rapid increase in the tumor pH value, reaching 7.0 within 60 minutes (Fig. 5B) and maintaining this value at least up to 6 hours (data not shown).

To evaluate the effects of pH buffering by PPI treatment, we at first assessed leukocyte infiltrate using an active immunotherapy approach. Mice bearing 7-day-old B16-OVA tumors were vaccinated with DC-OVA<sub>257-264</sub>, treated at the peak of the vaccine-induced immune response (i.e., day 3 postvaccine) with either PBS or one single PPI administration, and sacrificed 24 hours later. Leukocytes infiltrating the tumor mass were predominantly macrophages (CD11b), and to a lesser extent CD8<sup>+</sup> and CD4<sup>+</sup> T cells, B cells (CD19<sup>+</sup>B220<sup>+</sup>) and immature myeloid-derived cells (CD11b<sup>+</sup>Gr1<sup>+</sup>; Fig. 5C). Most CD4<sup>+</sup> and CD8<sup>+</sup> T cells were CD44<sup>+</sup>, confirming exposure to antigen (Fig. 5D and E). Treatment with PPI did not substantially modify the inflammatory infiltrate in this experimental setting (Fig. 5C–E). Because the limited number of endogenous CD8<sup>+</sup> T-cells infiltrating tumor lesions did not allow any functional analysis, a second experimental approach based on adoptive immunotherapy was introduced.

To this aim, mice bearing a 12-day-old melanoma (B16-OVA) were infused with activated CFSE-labeled CD44<sup>+</sup> OTI T cells, 24 hours later treated with PPI or PBS and sacrificed at day 14, according to the schedule depicted in Fig. 6A. As shown in Fig. 6B (left), a tendency toward a higher infiltration of CD8<sup>+</sup> T cells was observed in tumor lesions from mice receiving PPI with respect to PBS. However, the differences between the 2 groups

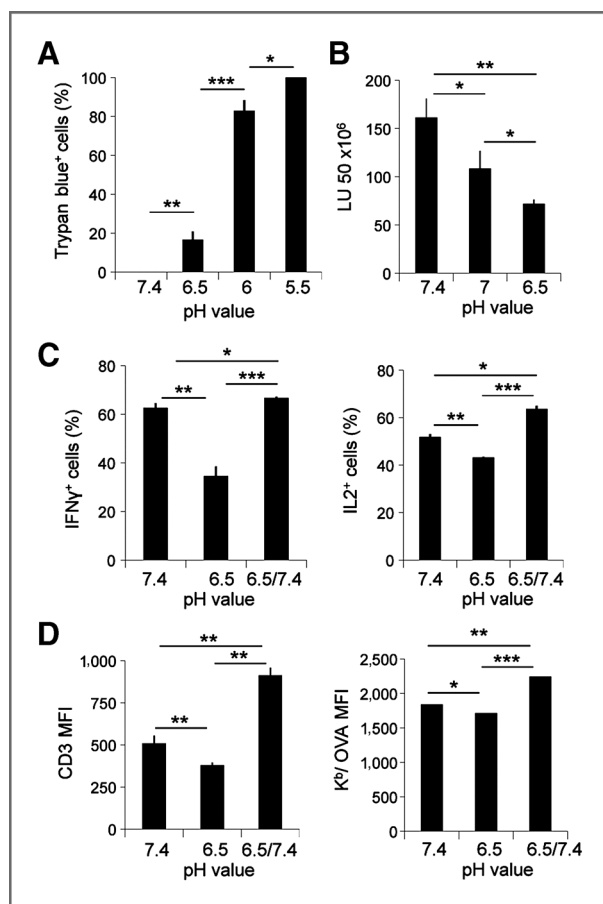


**Figure 4.** Low pH induces reversible anergy in mouse T lymphocytes. Activated OTI cells cultured at the indicate pH values were assessed for viability by trypan blue exclusion (A) or cytotoxic activity by <sup>51</sup>Cr release assay (B). Data represent mean  $\pm$  SD. C, OTI cells were assessed for IFN $\gamma$  (left) and IL-2 (right) production by intracellular staining. Data represent the percentage of CD8<sup>+</sup>CD44<sup>+</sup>IFN $\gamma$ <sup>+</sup> and CD8<sup>+</sup>CD44<sup>+</sup>IL-2<sup>+</sup> T cells. D, CD3 (left) and TCR (right) expression on CD8<sup>+</sup> T cells assessed by flow cytometry. MFI, mean fluorescence intensity. Lymphocytes restored to pH 7.4 for 24 hours before the assay were also included in the analysis (6.5/7.4 in C and D). Results are representative of at least 3 independent experiments. \*\*\*,  $P < 0.001$ ; \*\*,  $0.001 < P < 0.01$ ; \*,  $0.01 < P < 0.05$  (the Student  $t$  test).

were much more evident when the TIL activation state was assessed. Indeed, the number of CD44<sup>+</sup>CD8<sup>+</sup>IFN $\gamma$ <sup>+</sup> T cells per gram of tumor was statistically higher in PPI-treated animals (Fig. 6B, right). We then dissected the contribution of adoptively transferred versus endogenous T cells in this phenomenon by analyzing IFN $\gamma$  production in CFSE<sup>+</sup> or CFSE<sup>-</sup>CD44<sup>+</sup>CD8<sup>+</sup> T cells, respectively. As depicted in Fig. 6C, both the percentage and the absolute number of IFN $\gamma$ <sup>+</sup>CD44<sup>+</sup>CD8<sup>+</sup> TILs staining positive for CFSE and thus representing injected OTI cells, was enhanced in PPI with respect to PBS-treated mice. In addition, IFN $\gamma$  mean fluorescence intensity was also enhanced (Fig. 6D), suggesting a more efficient production on a per cell basis. In addition, and similarly to what reported in the *in vitro* experiments (Fig. 2C), CFSE<sup>+</sup> cells showed increased expression of p-ERK when isolated from PPI-treated tumors

(Supplementary Fig. S6B). Interestingly, a potentiated activation state could be also detected in CFSE<sup>-</sup> TILs from PPI-treated mice (Fig. 6E), indicating that endogenous TILs could benefit from a buffered pH milieu as well.

Because PPIs are prodrugs activated by protonation at low pH (28), their effect on resident lymphocytes should be selectively triggered by acidic environments, such as that displayed by tumor lesions (Fig. 5A). Accordingly, no sign of increased T-cell activation was detected in both CFSE<sup>+</sup> and CFSE<sup>-</sup>CD8<sup>+</sup>CD44<sup>+</sup> T cells subsets isolated from spleen (Fig. 6F), lung, and kidney (data not shown) from PPI-treated mice.

Finally, to evaluate *in vivo* effects of PPI on TIL functions also in a model of active immunotherapy, naive OTI cells were adoptively transferred in mice, subsequently challenged with B16-OVA cells and vaccinated with DC-OVA<sub>257-264</sub> with or without PPI treatment, according to the schedule detailed in Supplementary Fig. S7A. TIL analysis conducted in mice sacrificed at day 12 showed that treatment with PPI increased the ability of CD8<sup>+</sup> T cells, including OTI and endogenous CD8<sup>+</sup> T cells, to recognize OVA<sub>257-264</sub> peptide with higher affinity (with at least one log difference) with respect to the same cells derived from PBS-treated mice (Supplementary Fig. S7B).

#### PPI treatment increases the therapeutic potential of adoptive immunotherapy

To investigate the therapeutic potential of the combination of PPI treatment and immunotherapy, mice bearing an 8-day B16 or B16-OVA melanoma were treated according to the schedules detailed in Fig. 7. Esomeprazole was used at 12.5 mg/kg (Fig. 7A), which in dosing experiments (ranging from 1.25–600 mg/kg) was the highest tolerated dose, whereas activated OTI cells were administered in a single treatment at numbers ranging from 1 to 6  $\times 10^6$  cells, representing the best condition for antitumor effect (data not shown). Preliminary experiments were also conducted to identify the appropriate time schedule for PPI treatment after adoptive transfer. As reported in Supplementary Fig. S8, PPI treatment synergized with the adoptive transfer of lymphocytes when given either at the time of lymphocyte infusion or within the following 3 days. Later on the synergy diminished and was lost by day 9, likely due to the loss of adoptively transferred T cells (29). Hence, in a first set of experiments PPI was given at the time of adoptive transfer and repeated in the following days. Combined treatment with PPI and OTI cells at the doses mentioned earlier induced a statistically significant increase in animal survival, with a doubling in the overall survival rate relative to mice treated with PBS alone (Fig. 7A). Notably, equal tumor growth inhibition was achieved when PPI was administered before OTI adoptive transfer (Fig. 7B). The specificity of the treatment was confirmed by the finding that OTI cells and PPI did not impact on the survival of mice bearing B16 not expressing OVA (Fig. 7A, inset).

To test whether pH tumor buffering could improve the efficacy of nontransgenic T cells, splenocytes from mice previously sensitized against TRP-2 (19) were adoptively transferred into B16 melanoma-bearing mice (Fig. 7C).

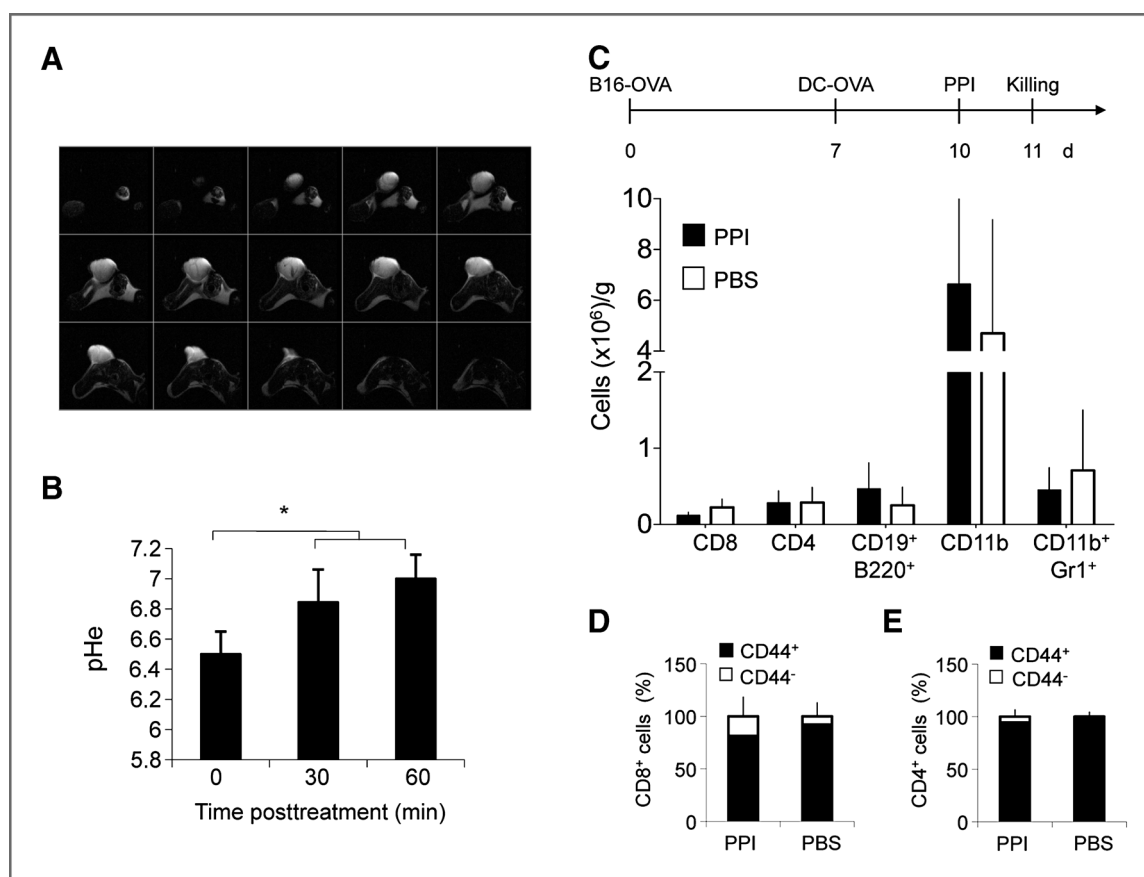


**Figure 5.** Characterization of the melanoma microenvironment before and after PPI treatment. **A**, MRI T2-weighted images of B16-OVA tumors. Fast spin echo multislice images were acquired with the following parameters: TR/TE<sub>eff</sub> = 3,000/60 ms; 2 transients; 15 slices; FOV, 30 × 30 mm<sup>2</sup>; matrix, 256 × 256; thickness = 1 mm (corresponding to in plane resolution of 0.1 × 0.1 mm<sup>2</sup>). Except for a few vessels, the tumor mass appeared homogeneous. **B**, tumor pH value was measured by MRS in animals engrafted with B16-OVA tumors ( $2 \times 10^5$  cells;  $n = 6$  from 3 different experiments) before (0 minute) and 30 and 60 minutes after i.p. infusion of PPI (12.5 mg/kg). Data are reported as mean  $\pm$  SD. \*,  $0.01 < P < 0.05$  (the Student *t* test). **C**, schematic representation of the experiment. Seven-day B16-OVA melanoma-bearing mice received DC-OVA<sub>257-264</sub> ( $5 \times 10^5$  cells intradermally), followed by i.p. administration of PPI ( $n = 5$ ) or PBS ( $n = 5$ ). Tumor cell suspensions obtained after 24 hours were analyzed for expression of the indicated markers by flow cytometry. Data are reported as the number of positive cells  $\pm$  SD per gram of tumor. The mean percentage  $\pm$  SD of CD8<sup>+</sup>CD44<sup>+</sup> (**D**) and CD4<sup>+</sup>CD44<sup>+</sup> (**E**) T cells is also reported. Each panel is representative of 3 independent experiments.

Mice were pretreated with nonmyeloablative total body irradiation (TBI; 600 rad) to favor *in vivo* expansion of the adoptively transferred T cells (2). PPI administration was applied as described in the treatment schedule (Fig. 7C). Interestingly, survival was significantly prolonged in mice receiving both TRP-2-specific T cells and PPI treatment as compared with mice treated only with adoptive T-cell transfer (Fig. 7C).

## Discussion

Here, we provide evidence that tumor acidity negatively regulates CD8<sup>+</sup> tumor-specific effector T cells in both human and murine experimental settings, and that systemic administration of esomeprazole restores physiologic pH at the tumor site and promotes a more efficient antitumor T-cell activity in melanoma-bearing mice. TILs cultured at pH values most frequently found in the tumor microenvironment (10, 11) reproducibly displayed reduced effector functions, coupled

with an inability to secrete IL-2, upregulate CD25, and activate STAT5/ERK signaling upon TCR activation. This is compatible with the induction of T-cell anergy (25, 26). Together with defects in perforin degranulation and cytokine secretion (30), these features are reminiscent of those detected in TILs analyzed *ex vivo* or in circulating CD3<sup>+</sup> T cells of advanced disease patients (3). Thus, acidity might indeed contribute to the dysfunction of tumor T-cell immunity observed in both mice and humans (31).

Microenvironmental acidosis, a near-universal property of solid cancers, is due in part to the upregulation of glycolysis and increased glucose consumption (7). Recent evidence has shown that mutations in crucial oncogenes, such as KRAS and BRAF, trigger the activation of glucose-related genes, leading to enhanced glycolysis in turn driving the acquisition of further mutations (32). These metabolic conditions, promoting acidity and additional biochemical alterations from the very initial steps of malignant transformation (33–35), could then act as selective forces in tumor microenvironment (7, 33–35).

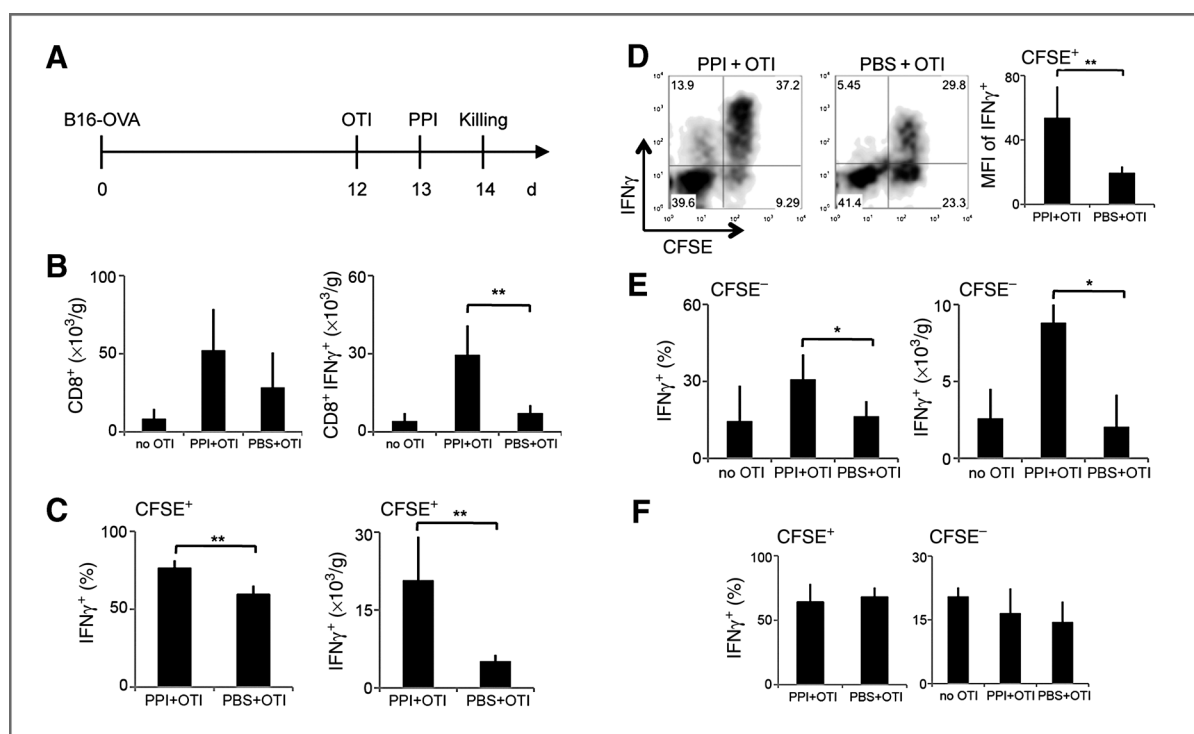


**Figure 6.** PPI treatment improves TIL effector function. **A**, schematic representation of the experiment. Mice were challenged s.c. with B16-OVA cells, and 12 days later, they were infused with activated and CFSE-labeled OTI cells ( $3 \times 10^5$ ). Mice receiving no adoptive transfer (no OTI;  $n = 3$ ) were introduced as negative control. One day after, animals were treated i.p. with esomeprazole (PPI + OTI;  $n = 5$ ) or PBS (PBS + OTI;  $n = 5$ ), and 24 hours later, tumor cell suspensions were assessed for intracellular cytokine release by flow cytometry. **B**, absolute numbers (cells/g) of  $CD8^+ CD44^+$  cells (left) and of  $CD8^+ IFN\gamma^+$  cells within the  $CD8^+ CD44^+$  subset (right) are reported. **C**, percentage (left) and absolute numbers (cells/g; right) of  $CD44^+ CD8^+ IFN\gamma^+$  cells within the CFSE<sup>+</sup> cell subset. **D**, representative plots of TILs (gated on  $CD8^+ CD44^+$  cells) for each experimental condition. Numbers refer to the percentage of cells in each quadrant. At right, mean fluorescence intensity of IFN $\gamma$  within the CFSE<sup>+</sup> cells is reported. **E**, percentage (left) and absolute numbers (cells/g; right) of  $CD44^+ CD8^+ IFN\gamma^+$  cells within the CFSE<sup>-</sup> cell subset. **F**,  $CD44^+ CD8^+ IFN\gamma^+$  cells within the CFSE<sup>+</sup> (left) and CFSE<sup>-</sup> (right) populations evaluated in the spleen of tumor-bearing mice that were treated or not with PPI. Data are representative of at least 3 independent experiments. Student *t* test: \*\*,  $0.001 < P < 0.01$ ; \*,  $0.01 < P < 0.05$ .

Our results support the hypothesis that acidity reduces T-cell performance by unbalancing the biochemical equilibrium required for physiologic activities, including proliferation, exocytosis, and secretion. In this scenario, specific cellular pathways might be more sensitive to pH variations than others. Perforin activation, for instance, is known to depend on short C-terminal peptide cleavage within acidic lysosome-like granules (36). As reported herein, microenvironmental acidity appears to perturb plasma membrane and microtubule mobility, leading to a less efficient association of different TCR components with CD8 or other coreceptors thereby contributing to T-cell anergy (4). It could be hypothesized that additional hypoxia-driven metabolic dysfunctions, causing extracellular adenosine accumulation (37), could act in synergy with acidic pH in dampening T-cell function through A2A adenosine receptor-driven cyclic AMP intracellular generation (38).

In our *in vitro* experiments, acidity-related T-cell anergy appeared to be reversible upon pH buffering, although longer exposure or lower pH values caused permanent damage and T-cell apoptosis. This implies that a portion of T-cell immunity might be lost at tumor sites characterized by extreme metabolic alterations. MRS analysis indi-

cated that pH buffering could be transiently achieved *in vivo* by proton pump inhibition. Similar results were previously attained in human melanoma xenografts (10), where the pH modulating effect of PPI was shown to persist no longer than 24 hours. Spatial heterogeneity of pH<sub>e</sub> within the tumor has been reported in human solid tumor xenografts and is expected to occur in a metabolically complex tumor environment (7, 11). B16-OVA tumors displayed a homogeneous structure, at least at the examined time points, suggesting that pH<sub>e</sub> might as well be rather homogeneous. However, we cannot exclude spatial distribution of pH<sub>e</sub> in localized regions which were not detectable with the settings used.

By exploiting the adoptive transfer of antigen-specific T cells, we found that *in vivo* pH buffering by PPI was reproducibly associated with ameliorated TIL recruitment and effector functions in melanoma lesions. Notably, this effect was extended also to endogenous T cells, suggesting that PPI-mediated pH restoration might contribute to the recovery of spontaneous immunity as well. Tumor lesions from PPI-treated mice receiving OTI cells did not show a dramatic increase of T-cell infiltration, but rather a strong boost in the activation state. Nevertheless, in all survival

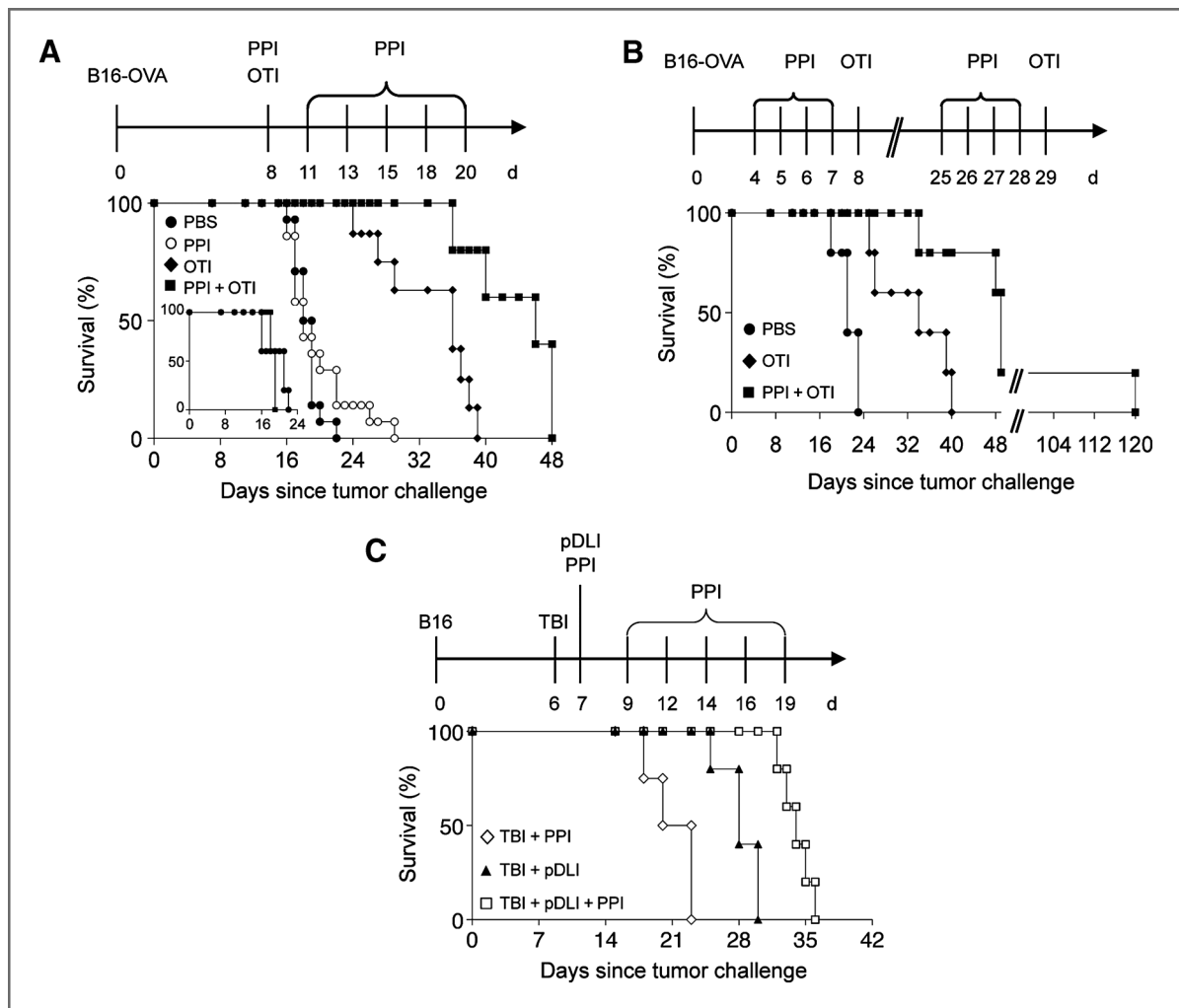


**Figure 7.** PPI treatment increases the therapeutic potential of adoptive immunotherapy. Eight-day B16-OVA or B16 melanoma-bearing mice were randomly assigned to either one of the treatment groups described in A to C (5–14 animals per group). A, treatments: PBS (black circles); PPI (open circles); activated OTI cells ( $6 \times 10^6$ /mouse; black diamonds), or PPI + OTI (black squares). Kaplan–Meier plot log-rank tests: PBS versus PPI,  $P = 0.459$ ; PBS versus OTI,  $P < 0.0001$ ; PBS versus PPI + OTI,  $P < 0.0001$ ; PPI versus OTI,  $P < 0.0002$ ; PPI versus PPI + OTI,  $P < 0.0002$ ; and OTI versus PPI + OTI,  $P < 0.001$ . Inset in A, as control, PPI + OTI (black squares) treatment was conducted in mice affected by B16 melanoma that did not express the OVA antigen; PBS (black circles). B, treatments: PBS (black circles); OTI cells (black diamonds), or PPI + OTI (black squares). Kaplan–Meier plot log-rank tests: PBS versus OTI,  $0.01 < P < 0.001$ ; PBS versus PPI + OTI,  $0.01 < P < 0.001$ ; and OTI versus PPI + OTI,  $0.05 < P < 0.01$ . C, treatments: TBI (600 rad) in combination with PPI (open diamonds); TBI plus adoptive transfer of splenocytes from mice presensitized against TRP-2 ( $60 \times 10^6$ /mouse; pDLI, black triangles); or TBI + pDLI + PPI (open squares). Kaplan–Meier plot log-rank tests: TBI + PPI versus TBI + pDLI,  $P = 0.004$ ; TBI + PPI versus TBI + pDLI + PPI,  $P = 0.0026$ ; and TBI + pDLI versus TBI + pDLI + PPI,  $P = 0.004$ .

experiments, pH buffering was able to significantly improve the therapeutic efficacy not only of adoptive immunotherapy but also of cancer vaccines, even based on natural melanoma antigens such as TRP-2. It could be speculated that PPI in combination with immunotherapy may enable effector T cells to locally trigger lymphocytes with different specificities through antigen spreading contributing to tumor control (39). This has been suggested to occur in human setting such as in patients with melanoma, where clinical efficacy of cancer vaccines can be achieved even in the presence of apparently low frequency of TIL in tumor regressing lesions (40). The buffering of tumor acidity may be also associated with other beneficial effects. Indeed, in addition to the boost

of IFN $\gamma$  release, T cells infiltrating PPI-treated tumors may improve granzyme and CD40L expression as well as pathways associated with therapeutically effective T-cell responses (41–43). Furthermore, PPI might directly correct biochemical alterations known to occur at TCR or MHC/peptide complex level (44, 45), thus strengthening T-cell/target interaction and improving tumor recognition and killing. In line with this hypothesis, we report that the TCR affinity for the cognate OVA peptide is improved in T cells collected from PPI-treated lesions. We can also easily foresee that buffering tumor acidity could improve the activity of other effector cells such as natural killer (NK) or natural killer T (NKT) cells, or reduce the negative impact of

regulatory populations ( $T_{reg}$  and MDSC), as presently under investigation.

Finally, PPI might represent a rather tumor selective immunomodulator, as they did not apparently affect T cells infiltrating normal tissues lacking acidic conditions, required for the prodrug transformation into its active sulfonamide form. The specificity of PPI for the low pH milieu might explain why these drugs can be administered at very high doses without significant toxicity, as occurs in the treatment of patients with Zollinger–Ellison syndrome (28) or in the currently ongoing clinical trials testing the combination of high-dose PPI with chemotherapy in patients with cancer (www.clinicaltrials.nih.gov).

Previous reports have shown that the hypoxic and/or metabolic pathways in cancer cells may contribute to tumor immune escape by rendering the tumor microenvironment hostile for normal cells (46, 47). The present study shows that acidity *per se* may represent a novel mechanism of immune escape, facilitating disease progression and invasion. In this view, pharmacologic tools restoring physiologic pH at tumor sites even transiently may represent a promising strategy for recovering specific immunity and improving the efficacy of adoptive and active immunotherapies in patients with cancer.

#### Disclosure of Potential Conflicts of Interest

No potential conflicts of interest were disclosed.

#### References

- Pages F, Kirilovsky A, Mlecnik B, Asslaber M, Tosolini M, Bindea G, et al. *In situ* cytotoxic and memory T cells predict outcome in patients with early-stage colorectal cancer. *J Clin Oncol* 2009;27:5944–51.
- Rosenberg SA, Dudley ME. Adoptive cell therapy for the treatment of patients with metastatic melanoma. *Curr Opin Immunol* 2009;21:233–40.
- Frey AB, Monu N. Signaling defects in anti-tumor T cells. *Immunol Rev* 2008;222:192–205.
- Demotte N, Stroobant V, Courtoy PJ, Van Der Smissen P, Colau D, Luescher IF, et al. Restoring the association of the T cell receptor with CD8 reverses anergy in human tumor-infiltrating lymphocytes. *Immunity* 2008;28:414–24.
- Kim PS, Ahmed R. Features of responding T cells in cancer and chronic infection. *Curr Opin Immunol* 2010;22:223–30.
- Parmiani G, Castelli C, Santinami M, Rivoltini L. Melanoma immunology: Past, present and future. *Curr Opin Oncol* 2007;19:121–7.
- Gatenby RA, Gillies RJ. Why do cancers have high aerobic glycolysis? *Nat Rev Cancer* 2004;4:891–9.
- Chiche J, Ilc K, Laferrière J, Trottier E, Dayan F, Mazure NM, et al. Hypoxia-inducible carbonic anhydrase IX and XII promote tumor cell growth by counteracting acidosis through the regulation of the intracellular pH. *Cancer Res* 2009;69:358–68.
- Supuran CT. Carbonic anhydrases: Novel therapeutic applications for inhibitors and activators. *Nat Rev Drug Discov* 2008;7:168–81.
- De Milioto A, Canese R, Marino ML, Borghi M, Iero M, Villa A, et al. pH-dependent antitumor activity of proton pump inhibitors against human melanoma is mediated by inhibition of tumor acidity. *Int J Cancer* 2010;127:207–19.
- Helmlinger G, Yuan F, Dellian M, Jain RK. Interstitial pH and pO<sub>2</sub> gradients in solid tumors *in vivo*: high-resolution measurements reveal a lack of correlation. *Nat Med* 1997;3:177–82.
- Kellum JA. Metabolic acidosis in patients with sepsis: Epiphenomenon or part of the pathophysiology? *Crit Care Resusc* 2004;6:197–203.
- Lardner A. The effects of extracellular pH on immune function. *J Leukoc Biol* 2001;69:522–30.
- Dudley ME, Wunderlich JR, Shelton TE, Even J, Rosenberg SA. Generation of tumor-infiltrating lymphocyte cultures for use in adoptive transfer therapy for melanoma patients. *J Immunother* 2003;26:332–42.
- Pilla L, Patuzzo R, Rivoltini L, Maio M, Pennacchioli E, Lamaj E, et al. A phase II trial of vaccination with autologous, tumor-derived heat-shock protein peptide complexes Gp96, in combination with GM-CSF and interferon-alpha in metastatic melanoma patients. *Cancer Immunol Immunother* 2006;55:958–68.
- UKCCCR guidelines for the use of cell lines in cancer research. *Br J Cancer* 2000;82:1495–509.
- Hogquist KA, Jameson SC, Heath WR, Howard JL, Bevan MJ, Carbone FR. T cell receptor antagonist peptides induce positive selection. *Cell* 1994;76:17–27.
- Ljunggren HG, Karre K. Host resistance directed selectively against H-2-deficient lymphoma variants. analysis of the mechanism. *J Exp Med* 1985;162:1745–59.
- Bellone M, Cantarella D, Castiglioni P, Crosti MC, Ronchetti A, Moro M, et al. Relevance of the tumor antigen in the validation of three vaccination strategies for melanoma. *J Immunol* 2000;165:2651–6.
- Boni A, Iezzi G, Degl'Innocenti E, Grioni M, Jachetti E, Camporeale A, et al. Prolonged exposure of dendritic cells to maturation stimuli favors the induction of type-2 cytotoxic T lymphocytes. *Eur J Immunol* 2006;36:3157–66.
- Rotzschke O, Falk K, Stevanovic S, Jung G, Walden P, Rammensee HG. Exact prediction of a natural T cell epitope. *Eur J Immunol* 1991;21:2891–4.
- Bloom MB, Perry-Lalley D, Robbins PF, Li Y, el-Gamil M, Rosenberg SA, et al. Identification of tyrosinase-related protein 2 as a tumor rejection antigen for the B16 melanoma. *J Exp Med* 1997;185:453–9.

#### Authors' Contributions

**Conception and design:** A. Calcinotto, P. Filipazzi, M. Iero, G. Parmiani, S. Fais, M. Bellone, L. Rivoltini

**Development of methodology:** A. Calcinotto, P. Filipazzi, M. Grioni, M. Iero, L. Generoso, S. Fais, M. Bellone

**Acquisition of data (provided animals, acquired and managed patients, provided facilities, etc.):** A. Calcinotto, P. Filipazzi, M. Grioni, M. Iero, M. De Milioto, A. Ricupito, A. Cova, R. Canese, E. Jachetti, M. Rossetti, M. Borghi, S. Fais

**Analysis and interpretation of data (e.g., statistical analysis, biostatistics, computational analysis):** A. Calcinotto, P. Filipazzi, M. Iero, M. De Milioto, A. Cova, R. Canese, M. Rossetti, G. Parmiani, S. Fais, M. Bellone, L. Rivoltini

**Writing, review, and/or revision of the manuscript:** A. Calcinotto, P. Filipazzi, M. De Milioto, R. Canese, V. Huber, S. Fais, M. Bellone, L. Rivoltini

**Administrative, technical, or material support (i.e., reporting or organizing data, constructing databases):** A. Calcinotto, A. Cova

**Study supervision:** M. Santinami, S. Fais, M. Bellone, L. Rivoltini

**Interpretation and discussion of data:** V. Huber

#### Acknowledgments

The authors thank M.P. Protti (San Raffaele Scientific Institute) and C. Castelli (Fondazione IRCCS Istituto Nazionale Tumori) for manuscript; R. Longhi (CNR, Milan, Italy) for providing reagents. A. Calcinotto conducted this study in partial fulfillment of her Ph.D. at San Raffaele University.

#### Grant Support

The study was supported by grants from the Italian Association for Cancer Research (AIRC, Milan; AIRC ISS grant #5940), the Ministry of Health (Rome, Italy), the Ministry of University and Research (Rome, Italy), and the European Community.

The costs of publication of this article were defrayed in part by the payment of page charges. This article must therefore be hereby marked *advertisement* in accordance with 18 U.S.C. Section 1734 solely to indicate this fact.

Received April 19, 2011; revised February 29, 2012; accepted March 21, 2012; published OnlineFirst May 16, 2012.

23. Garcia-Hernandez Mde L, Gray A, Hubby B, Kast WM. *In vivo* effects of vaccination with six-transmembrane epithelial antigen of the prostate: a candidate antigen for treating prostate cancer. *Cancer Res* 2007;67:1344–51.
24. Otten GR, Germain RN. Split anergy in a CD8<sup>+</sup> T cell: receptor-dependent cytotoxicity in the absence of interleukin-2 production. *Science* 1991;251:1228–31.
25. Grundstrom S, Dohlsten M, Sundstedt A. IL-2 unresponsiveness in anergic CD4<sup>+</sup> T cells is due to defective signaling through the common gamma-chain of the IL-2 receptor. *J Immunol* 2000;164:1175–84.
26. Wells AD, Walsh MC, Sankaran D, Turka LA. T cell effector function and anergy avoidance are quantitatively linked to cell division. *J Immunol* 2000;165:2432–43.
27. Whiteside TL. Down-regulation of zeta-chain expression in T cells: a biomarker of prognosis in cancer? *Cancer Immunol Immunother* 2004;53:865–78.
28. Mullin JM, Gabello M, Murray LJ, Farrell CP, Bellows J, Wolov KR, et al. Proton pump inhibitors: actions and reactions. *Drug Discov Today* 2009;14:647–60.
29. Gattinoni L, Klebanoff CA, Restifo NP. Pharmacologic induction of CD8<sup>+</sup> T cell memory: better living through chemistry. *Sci Transl Med* 2009;1:11ps12.
30. Radoja S, Saio M, Schaer D, Koneru M, Vukmanovic S, Frey AB. CD8 (+) tumor-infiltrating T cells are deficient in perforin-mediated cytolytic activity due to defective microtubule-organizing center mobilization and lytic granule exocytosis. *J Immunol* 2001;167:5042–51.
31. Rabinovich GA, Gabrilovich D, Sotomayor EM. Immunosuppressive strategies that are mediated by tumor cells. *Annu Rev Immunol* 2007;25:267–96.
32. Yun J, Rago C, Cheong I, Pagliarini R, Angenendt P, Rajagopalan H, et al. Glucose deprivation contributes to the development of KRAS pathway mutations in tumor cells. *Science* 2009;325:1555–9.
33. Cairns RA, Harris IS, Mak TW. Regulation of cancer cell metabolism. *Nat Rev Cancer* 2011;11:85–95.
34. Vander Heiden MG, Cantley LC, Thompson CB. Understanding the warburg effect: The metabolic requirements of cell proliferation. *Science* 2009;324:1029–33.
35. Singer K, Kastenberger M, Gottfried E, Hammerschmied CG, Büttner M, Aigner M, et al. Warburg phenotype in renal cell carcinoma: high expression of glucose-transporter 1 (GLUT-1) correlates with low CD8<sup>+</sup> T-cell infiltration in the tumor. *Int J Cancer* 2011;128:2085–95.
36. Konjar S, Sutton VR, Hoves S, Repnik U, Yagita H, Reinheckel T, et al. Human and mouse perforin are processed in part through cleavage by the lysosomal cysteine proteinase cathepsin L. *Immunology* 2010;131:257–67.
37. Deaglio S, Dwyer KM, Gao W, Friedman D, Ushuva A, Erat A, et al. Adenosine generation catalyzed by CD39 and CD73 expressed on regulatory T cells mediates immune suppression. *J Exp Med* 2007;204:1257–65.
38. Sitkovsky MV, Kjaergaard J, Lukashev D, Ohta A. Hypoxia-adenosine immunosuppression: tumor protection by T regulatory cells and cancerous tissue hypoxia. *Clin Cancer Res* 2008;14:5947–52.
39. Corbière V, Chapiro J, Stroobant V, Ma W, Lurquin C, Lethé B, et al. Antigen spreading contributes to MAGE vaccination-induced regression of melanoma metastases. *Cancer Res* 2011;71:1253–62.
40. Lonchay C, van der Bruggen P, Connerotte T, Hanagiri T, Coulié P, Colau D, et al. Correlation between tumor regression and T cell responses in melanoma patients vaccinated with a MAGE antigen. *Proc Natl Acad Sci U S A* 2004;101:14631–8.
41. Connerotte T, Van Pel A, Godelaine D, Tartour E, Schuler-Thurner B, Lucas S, et al. Functions of Anti-MAGE T-cells induced in melanoma patients under different vaccination modalities. *Cancer Res* 2008;68:3931–40.
42. Ahmed N, Gottschalk S. How to design effective vaccines: lessons from an old success story. *Expert Rev Vaccines* 2009;8:543–6.
43. Gaucher D, Therrien R, Kettaf N, Angermann BR, Boucher G, Filali-Mouhim A, et al. Yellow fever vaccine induces integrated multi-lineage and polyfunctional immune responses. *J Exp Med* 2008;205:3119–31.
44. Molon B, Ugel S, Del Pozzo F, Soldani C, Zilio S, Avella D, et al. Chemokine nitration prevents intratumoral infiltration of antigen-specific T cells. *J Exp Med* 2011;208:1949–62.
45. Nagaraj S, Gupta K, Pisarev V, Kinarsky L, Sherman S, Kang L, et al. Altered recognition of antigen is a mechanism of CD8<sup>+</sup> T cell tolerance in cancer. *Nat Med* 2007;13:828–35.
46. Fischer K, Hoffmann P, Voelkl S, Meidenbauer N, Ammer J, Edinger M, et al. Inhibitory effect of tumor cell-derived lactic acid on human T cells. *Blood* 2007;109:3812–9.
47. Henning T, Kraus M, Brischwein M, Otto AM, Wolf B. Relevance of tumor microenvironment for progression, therapy and drug development. *Anti-cancer Drugs* 2004;15:7–14.

# Cancer Research

The Journal of Cancer Research (1916–1930) | The American Journal of Cancer (1931–1940)

## Modulation of Microenvironment Acidity Reverses Anergy in Human and Murine Tumor-Infiltrating T Lymphocytes

Arianna Calcinotto, Paola Filipazzi, Matteo Gironi, et al.

*Cancer Res* 2012;72:2746-2756. Published OnlineFirst May 16, 2012.

<b>Updated version</b>	Access the most recent version of this article at: doi: <a href="https://doi.org/10.1158/0008-5472.CAN-11-1272">10.1158/0008-5472.CAN-11-1272</a>
<b>Supplementary Material</b>	Access the most recent supplemental material at: <a href="http://cancerres.aacrjournals.org/content/suppl/2012/06/29/0008-5472.CAN-11-1272.DC1">http://cancerres.aacrjournals.org/content/suppl/2012/06/29/0008-5472.CAN-11-1272.DC1</a>

<b>Cited articles</b>	This article cites 47 articles, 20 of which you can access for free at: <a href="http://cancerres.aacrjournals.org/content/72/11/2746.full#ref-list-1">http://cancerres.aacrjournals.org/content/72/11/2746.full#ref-list-1</a>
<b>Citing articles</b>	This article has been cited by 24 HighWire-hosted articles. Access the articles at: <a href="http://cancerres.aacrjournals.org/content/72/11/2746.full#related-urls">http://cancerres.aacrjournals.org/content/72/11/2746.full#related-urls</a>

<b>E-mail alerts</b>	<a href="#">Sign up to receive free email-alerts</a> related to this article or journal.
<b>Reprints and Subscriptions</b>	To order reprints of this article or to subscribe to the journal, contact the AACR Publications Department at <a href="mailto:pubs@aacr.org">pubs@aacr.org</a> .
<b>Permissions</b>	To request permission to re-use all or part of this article, use this link <a href="http://cancerres.aacrjournals.org/content/72/11/2746">http://cancerres.aacrjournals.org/content/72/11/2746</a> . Click on "Request Permissions" which will take you to the Copyright Clearance Center's (CCC) Rightslink site.